

Article

Irrigation Salinity Affects Water Infiltration and Hydraulic Parameters of Red Soil

Shuai Tan ^{1,2,3,†}, Xinyue Su ^{1,2,†}, Xi Jiang ³, Wangxing Yao ^{1,2}, Shaomin Chen ^{1,2,*}, Qiliang Yang ^{1,2,*} and Songrui Ning ^{4,*} 

¹ Faculty of Modern Agricultural Engineering, Kunming University of Science and Technology, Kunming 650500, China; tans90@163.com (S.T.)

² Yunnan Provincial Field Scientific Observation and Research Station on Water-Soil-Crop System in Seasonal Arid Region, Kunming University of Science and Technology, Kunming 650500, China

³ College of Water Resources and Civil Engineering, Hunan Agricultural University, Changsha 410128, China

⁴ State Key Laboratory of Eco-Hydraulics in Northwest Arid Region of China, Xi'an University of Technology, Xi'an 710048, China

* Correspondence: chenshaomin1989@163.com (S.C.); yangqilianglovena@163.com (Q.Y.); ningsongrui@163.com (S.N.)

† These authors contributed equally to this work.

Abstract: Unconventional water resources (e.g., saline water, etc.) for irrigation as a promising supplementary water source can alleviate the freshwater shortage in the agriculture of red soil areas in Southern China. It should be noted that the presence of soluble salt in this water source may have detrimental influences on soil water infiltration and crop growth. Understanding the effect of unconventional water irrigation (UWI) on water infiltration in red soil is important. Previous studies have shown that the salinity of UWI can alter soil hydraulic properties to change soil water movement in saline soils. However, the underlying mechanism and factors of water infiltration in red soil under UWI with different salinity levels remain limited. Therefore, a laboratory experiment (one-dimensional vertical infiltration experiment and centrifuge method) was conducted to evaluate the effect of UWI with different salinity levels [0 (the distilled water, CK), 1 (S1), 2 (S2), 3 (S3), 5 (S5), and 10 (S10) g L⁻¹] on the soil water infiltration process, soil water characteristic curve (SWCC), soil water constants estimated using the SWCC, saturated and unsaturated hydraulic conductivity (K_S and K) as well as the soil chemistry of soil profile [pH, electrical conductivity (EC), and Na⁺ and Cl⁻ contents]. The primary factors of soil water infiltration were identified using stepwise regression and path analysis methods. The results showed that UWI salinity decreased water infiltration by 1.53–7.99% at the end of infiltration in red soil, following the order of CK > S1 > S5 > S2 > S3 > S10. Moreover, UWI could enhance soil water availability with an increase of 8.55–12.68% in available water capacity. In contrast, lower K_S and K were observed in S1–S10, and there was a negative linear relationship between irrigation salinity and K_S . UWI also produced the EC, Na⁺, and Cl⁻ accumulations in the soil profile. As the salinity level of UWI increased, the accumulations aggravated. Soil acidification was found in S1–S5, while soil alkalization was observed in S10. Additionally, α , PWP, and K_S were the primary factors influencing the water infiltration of red soil. This study can help optimize the soil infiltration model under UWI and establish a foundation for unconventional water management in the red soil regions of Southern China and other similar regions. In addition, the undisturbed red soil under agricultural unconventional water irrigation and the long-term effect of unconventional water application should be considered.

Keywords: irrigation salinity; soil water infiltration; soil water characteristics curve; soil hydraulic conductivity; red soil



Citation: Tan, S.; Su, X.; Jiang, X.; Yao, W.; Chen, S.; Yang, Q.; Ning, S. Irrigation Salinity Affects Water Infiltration and Hydraulic Parameters of Red Soil. *Agronomy* **2023**, *13*, 2627. <https://doi.org/10.3390/agronomy13102627>

Academic Editors: Anna Tedeschi and Belen Gallego-Elvira

Received: 25 August 2023

Revised: 9 October 2023

Accepted: 13 October 2023

Published: 17 October 2023



Copyright: © 2023 by the authors. Licensee MDPI, Basel, Switzerland. This article is an open access article distributed under the terms and conditions of the Creative Commons Attribution (CC BY) license (<https://creativecommons.org/licenses/by/4.0/>).

1. Introduction

The majority of Southern China has a subtropical monsoon climate, where rainfall distribution is extremely erratic, and seasonal drought is evident (e.g., most of the pre-

precipitation is mainly concentrated from April to June, accounting for half of the annual precipitation amount) [1,2]. Acid red soil is widely distributed in Southern China, covering an area of approximately 1.28×10^7 km² with a high production potential for agriculture [3]. However, this region is extraordinarily vulnerable to seasonal drought due to inadequate soil water availability and storage capacity. Additionally, the freshwater scarcity and the imbalance between supply and demand have intensified in agriculture because of global-warming-induced drought, serious water pollution, and increased demand for high-quality water driven by urban and industrial sectors [4]. Therefore, irrigated agriculture faces the challenge of using less water [5]. Finding alternative water sources to overcome freshwater scarcity is necessary for agriculture in Southern China.

Unconventional water resources (e.g., saline water, wastewater, agricultural drainage water, reclaimed water, etc.) have been increasingly addressed as potential alternatives to improve freshwater resource scarcity in agricultural irrigation in recent years [6–9]. These water resources have been considered as any water resources other than freshwater, and their global annual usage is 255 km³ [10]. Hence, the utilization of unconventional water resources as supplementary irrigation sources has the potential to mitigate the freshwater shortage in the agriculture of Southern China. However, these alternative sources usually contain many soluble salts. As a result, compared to freshwater irrigation, higher salinity (total salt content) and sodicity (sodium content) have been found in the soil under unconventional water irrigation (UWI). Maintaining physical soil properties to ensure adequate soil permeability for meeting crop water and leaching requirements is a crucial factor that needs to be considered to achieve sustainable and secure unconventional water application [5]. UWI could bring salt into the soil, which may damage soil structure [11], alter the water infiltration process in red soil [12], and further adversely affect crop growth [6,13,14]. Therefore, it is essential to understand the effect of UWI on water infiltration performance and its mechanism in red soil to enhance unconventional water use efficiency and mitigate its hazards in Southern China [15].

UWI significantly affects soil water infiltration, and these effects are related to its salinity [16]. Generally, lower salinity could promote soil water infiltration in saline soil, whereas a higher salinity exerts a negative impact. For instance, Zhang and Shen [17] analyzed water and salt transport in salinized soil under four treatments of brackish water irrigation (0, 1.7, 3.4, and 5.1 g L⁻¹) through a soil column experiment. They found that brackish water irrigation promoted soil water infiltration and hydraulic conductivity (K), and the shortest duration of infiltration was observed in the 30 cm soil column under irrigation water salinity of 5.1 g L⁻¹, which was only 6.25% of the infiltration time for the treatment of 0 g L⁻¹. However, there is a difference between saline soil and acid soil. Zhu et al. [18] observed that in comparison to distilled water (0.03 mS cm⁻¹), reclaimed water (<1.66 mS cm⁻¹) decreased cumulative infiltration in acid red soil, and the largest reduction of 85.71% occurred under irrigation with undiluted reclaimed water (1.66 mS cm⁻¹). Wu et al. [12] investigated the infiltration of acid red soil under irrigation with reclaimed water (<1.66 mS cm⁻¹) and found that the short-term application of raw reclaimed water resulted in a decrease in cumulative infiltration in red soil and also reduced the infiltration of aquic soil at different degrees.

Soil hydraulic parameters, including the soil water characteristic curve (SWCC), saturated hydraulic conductivity (K_s), and unsaturated hydraulic conductivity (K), play an essential role in water-related applications like agricultural irrigation. Understanding the effect of salinity on these parameters can help predict soil water movement under UWI for agriculture. Regarding the SWCC, salinity could affect soil retention and its characteristic parameters (such as soil water saturation content θ_s , residual water content θ_r , and shape parameters α , n , and m). Rezaei et al. [19] found that compared to freshwater (0.34 mS cm⁻¹), saline water (35.6 mS cm⁻¹) increased θ_s and n by up to 24% and 23% in alkaline soils, respectively, with an α decline of up to 8-fold, whereas θ_r varied inconsistently, from a decrease of 50% to an increase of 400%. Furthermore, Chaudhari [20] indicated that the K_s of clay, clay loam, and silt loam soils decreased drastically by 82.5%, 79.2%, and

93.9%, respectively, when the sodium adsorption ratio of irrigation water rose from 2.5 to 30 $\text{mmol}^{0.5} \text{L}^{-0.5}$. Likewise, Tarchouna et al. [16] performed a two-year experiment on sand soil under long-term UWI (1.31–1.54 mS cm^{-1}), revealing that K_S and K decreased considerably, with K_S at a soil depth of 30 cm dropping to only 16.75% of that for the non-irrigated sand soil. Conversely, Amini et al. [21] demonstrated that UWI had no significant effects on the K_S of clay soil via inverse modeling.

Soil hydraulic parameters can influence the medium transportation and transformation processes of water in soils [22]. Previous studies [23–29] stated that hydraulic conductivity (K_S and K) and the SWCC parameters (θ_s , α , n , and m) are the key factors of soil water flow. Fan et al. [23] reported that K_S had a significant influence on cumulative infiltration, with a 46-fold reduction in infiltration duration when K_S increased from 0.0043 to 0.2432 cm min^{-1} . According to sensitivity analysis of soil hydraulic parameters on unsaturated water flow, K_S , θ_s , α , n , and m had different contributions to soil infiltration. For example, Wang et al. [24] found that K_S , θ_s , and n significantly affected soil water, and the range of cumulative infiltration was above 10%. Huo and Jin [25] demonstrated that K_S , θ_s , and n produced a higher contribution to water flow as a single factor, and K_S and n had a positive effect on soil water infiltration. Stothoff [26] examined the sensitivity of a bare soil simulator using an effective semi-infinite column and revealed that the reduction in air entry pressure (the inverse of α) could promote long-term average net infiltration for homogeneous media. Wang et al. [27] also pointed out that the infiltration rate increased with the decreasing of the air pressure head (i.e., α increased), which was attributed to soil air escape from the surface at the air pressure head reaching an air-breaking value. Pan et al. [28] concluded that α as an independent input parameter was a major contributor to soil water flow by using sample-based regression and decomposition methods. Maina and Siirila-Woodburn [29] also found that vertical K and α mainly controlled the upward flow in the unsaturated soil profile using a global sensitivity analysis. Additionally, numerous studies have noted that UWI could accumulate soil salinity [30–32] and change soil pH [33,34], further affecting soil hydraulic properties.

In summary, UWI can alter the soil infiltration process by affecting soil hydraulic parameters such as SWCC, K_S , and K , as well as soil chemistry (pH, EC, and ion accumulation). Furthermore, the variations in soil hydraulic parameters and soil chemistry can be associated with the salinity level of irrigation water. However, the knowledge of the effects of salinity of UWI on soil physic and hydraulic parameters is still limited [35], hindering the use of unconventional water for agricultural irrigation, particularly in the red soils of Southern China. Therefore, we carried out a one-dimensional vertical infiltration experiment with five different salinity levels of simulated unconventional water (1, 2, 3, 5, and 10 g L^{-1}) and distilled water (CK, 0 g L^{-1}) to determine how the water infiltration process responded to the salinity level of UWI in red soil. Additionally, the mechanism of irrigation salinity on water infiltration was also analyzed using soil hydraulic parameters (SWCC, K_S , and K) and soil chemistry (pH, EC, and Na^+ and Cl^- contents) as indicators. This study could provide a scientific foundation for optimizing UWI practices and their utilization in red soil.

2. Materials and Methods

2.1. Soil Sample Preparation

The experimental soil was adopted as a typical red soil, obtained from Changsha County, Hunan Province (113°16'46" E, 28°32'49" N, Figure 1), where the land use is dry land. After removing dead branches, stones, and other debris on the soil surface, the soil of the tillage layer (0–20 cm) was sampled. Then, the red soil was air-dried and passed through a 2 mm sieve. According to the international soil classification system, the experimental red soil was classified as clay soil with 12% sand, 32% silt, and 56% clay. The average dry bulk density in the tillage layer was 1.24 g cm^{-3} , using a cutting ring method. The initial water content of the experimental red soil was 0.063 $\text{cm}^3 \text{cm}^{-3}$. The initial Na^+ and Cl^-

contents of the soil were 0.068 g kg^{-1} and 0.058 g kg^{-1} , respectively. The initial soil EC was 0.03 ms cm^{-1} , and the pH was 4.33.

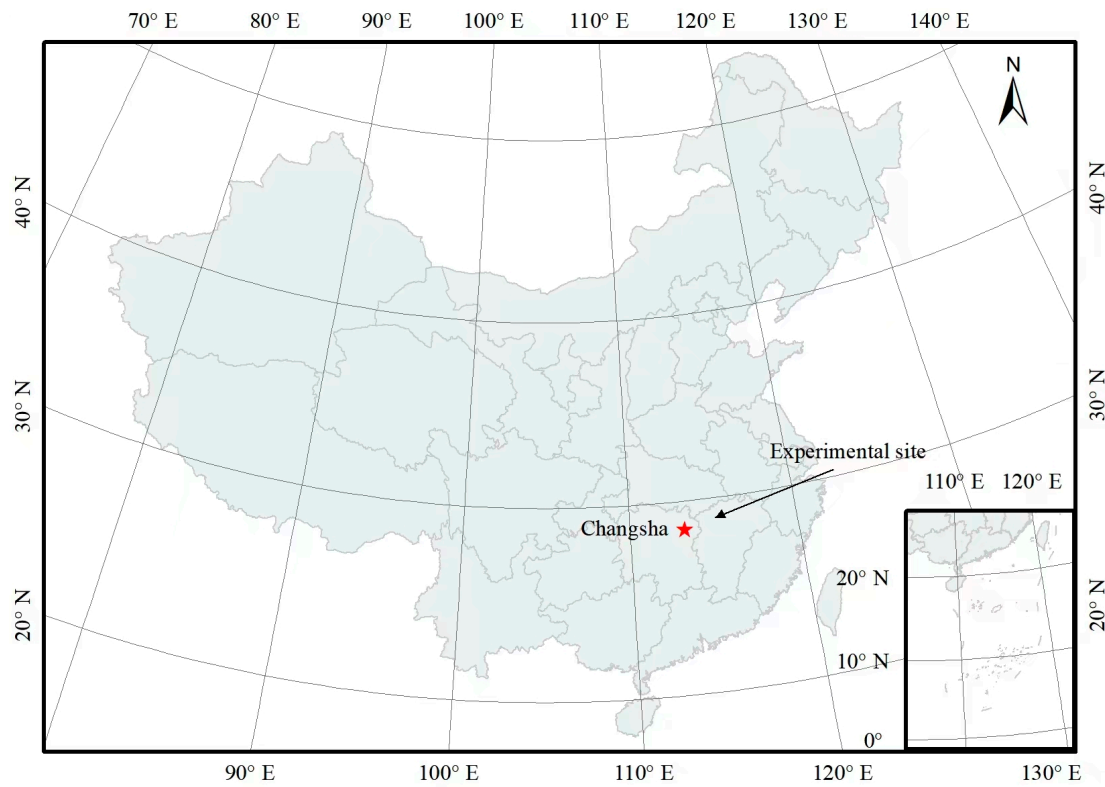


Figure 1. The location of the experimental soil sample.

2.2. Experimental Design

2.2.1. Experimental Treatment

Considering that Na^+ and Cl^- are the main solutes in unconventional water [36], and simplifying the effect of various ionic interactions on water infiltration in red soils, the experimental water was prepared with distilled water and analytically pure NaCl. Five salinity levels were set, i.e., 1, 2, 3, 5, and 10 g L^{-1} , denoted as S1, S2, S3, S5, and S10, respectively. The distilled water was set as a control (CK). The details of the treated water (S1–S10) and the CK are shown in Table 1.

Table 1. The salinity, electrical conductivity, and pH of the experimental irrigation water.

Treatment	Salinity (g L^{-1})	Electrical Conductivity (mS cm^{-1})	pH
CK	0	0.03 ± 0.01	6.88 ± 0.01
S1	1	2.03 ± 0.02	6.03 ± 0.04
S2	2	3.33 ± 0.02	6.07 ± 0.06
S3	3	4.59 ± 0.04	6.05 ± 0.07
S5	5	7.09 ± 0.03	6.03 ± 0.03
S10	10	12.80 ± 0.07	5.91 ± 0.05

2.2.2. One-Dimensional Vertical Infiltration Experiment

A one-dimensional vertical infiltration experiment under a constant head was conducted to observe the water infiltration process in red soil under UWI with five salinity levels of unconventional water (S1–S10) and a CK. The experimental device consisted of soil columns and water supply equipment. The soil column was made of cylindrical plexiglass with an 8 cm inner diameter and a 50 cm height. A Mariotte bottle (5 cm in inner diameter and 50 cm in height) was used as the water supply equipment to stabilize the water head

above the surface of the soil column. The bottom of the soil column was covered with gauze and filter paper to prevent the loss of soil particles. The soil column was uniformly filled with disturbed red soil in nine layers of 5 cm thickness and scratched between layers. The dry bulk density of loading red soil was set as 1.24 g cm^{-3} (i.e., a soil mass of 0.311 kg per 5 cm of soil layer) to eliminate the interference of soil structure and approach the actual soil conditions. After filling, the soil column surface was covered with filter paper to avoid inlet water disturbance. The water head was maintained at about 2 cm during the experiment period [37]. To avoid the effect of the bottom boundary of the soil column, the water level of the Mariotte bottle and the infiltration duration were recorded for each treatment until the wetting front in the soil column reached 35 cm. At the end of the one-dimensional vertical infiltration experiment, the water supply was stopped, and then the ponded water on the soil surface was quickly removed. Soil samples were collected using a soil auger with a 3 cm inner diameter from the soil surface to the wetting front at a 5 cm interval. After drying in an oven at $105 \pm 2 \text{ }^\circ\text{C}$ for 24 h, the EC and pH of the soil solution (1:5, soil/water) were measured using a Mettler Seven Excellence S470-B multifunctional tester (Mettler Toledo, Schwerzenbach, Switzerland). Na^+ and Cl^- concentrations were determined using a PXSJ-316F ion meter (Shanghai Yidian Scientific Instruments Co., Ltd., Shanghai, China) and then were converted to Na^+ and Cl^- contents of the soil according to solution volume and soil mass. Each treatment was repeated four times with four soil columns, therefore there were twenty-four soil columns in total.

2.2.3. Soil Water Characteristic Curve (SWCC) Measurement

The SWCC was determined using a high-speed refrigerated centrifuge (CR21N, Hitachi Ltd., Tokyo, Japan). The air-dried red soil was loaded into the matching cutting rings (100 cm^3 in volume) of the centrifuge with a dry bulk density of 1.24 g cm^{-3} , and the filter paper was covered at the bottom of these cutting rings to prevent the loss of soil particles. Subsequently, these cutting rings were, respectively, placed into the treated water (S1–S10) and the CK to saturate from bottom to top for 24 h and were weighed on an electronic balance with a precision of 0.01 g. These cutting rings containing saturated soil were placed in particular tubes. Next, these tubes were placed into the centrifuge to gradually dehydrate at a temperature of $20 \text{ }^\circ\text{C}$ from a low rotation speed to a high rotation speed to reach a specific soil suction (0, 51, 102, 204, 306, 408, 612, 816, 1020, 1530, 2040, 3060, 4080, 6120, 8160, 10,200, and 15,300 cm) and were weighed. At the end of dehydration, the soil samples were dried in a fan-assisted oven to a constant weight of $105 \pm 2 \text{ }^\circ\text{C}$ for 24 h to calculate soil gravimetric water content. The soil volumetric water content (SWC) at each soil suction was converted by multiplying the soil gravimetric water content and dry bulk density. The SWCC could be expressed using the relationship between the soil suction and SWC. Each treatment had four replicates.

2.2.4. Saturation Hydraulic Conductivity Measurement

The saturated hydraulic conductivity (K_S) of red soil for S1–S10 and the CK was determined with the constant water head method. Similar to the infiltration experiment, a Mariotte bottle was used to maintain the water head. After being saturated with corresponding irrigation water from the bottom to the top for 24 h, the soil samples were leached using a Mariotte bottle at a 2 cm water head for each treatment [19]. The outflow was collected every 30 min until it reached a steady state (the parallel error did not exceed 2%). There were four replicates for each treatment.

2.3. Mathematical Model of Soil Water Infiltration and Hydraulic Properties

2.3.1. One-Dimension Vertical Infiltration Model

Philip [38] proposed that there is a power function relationship between cumulative infiltration (I , cm) and infiltration duration (t , min). As soil matric potential is dominant in the short duration of infiltration, the Philip equation can be expressed as follows:

$$I = S t^{0.5} \quad (1)$$

where S is soil sorptivity ($\text{cm min}^{-0.5}$), which reflects soil infiltration capacity.

2.3.2. van Genuchten Model

van Genuchten [39] reported a model (VG model) that can accurately describe the SWCC. The VG model is given as follows:

$$\theta = \begin{cases} \theta_r + \frac{\theta_s - \theta_r}{[1 + (\alpha h)^n]^m} & h < 0 \\ \theta_s & h \geq 0 \end{cases} \quad (2)$$

where θ is the soil volumetric water content ($\text{cm}^3 \text{cm}^{-3}$), θ_s is the soil saturated water content ($\text{cm}^3 \text{cm}^{-3}$) (which was determined from the SWCC experiment), θ_r is the residual water content ($\text{cm}^3 \text{cm}^{-3}$), and θ_r was set to the initial soil water ($0.063 \text{cm}^3 \text{cm}^{-3}$) to better investigate the effects of irrigation salinity on the SWCC parameters. h is soil suction (cm), α is the inverse of the air-entry value (cm^{-1}), and n and m are parameters that affect the shape of the SWCC ($m = 1 - 1/n$).

2.3.3. Saturated Hydraulic Conductivity Calculation

Saturated hydraulic conductivity (K_S , cm min^{-1}) is calculated using Darcy's law [40], which is expressed as follows:

$$K_S = \frac{QL}{At\Delta H} \quad (3)$$

where Q is the volume of the outflow through the soil column (mL), L is the infiltration length (cm), A is the cross-sectional area of the soil column (cm^2), t is the time interval (min), and ΔH is the head difference across the flow path (cm).

2.3.4. Unsaturated Hydraulic Conductivity Model

Combining the VG model with the pore-size distribution model of Mualem, the K function can be written as follows [41]:

$$K(\Theta) = K_S \Theta^l \left[1 - \left(1 - \Theta^{1/m} \right)^m \right]^2 \quad (4)$$

where $K(\Theta)$ is the unsaturated hydraulic conductivity at an effective degree of saturation (cm min^{-1}), Θ is the effective degree of saturation (which is expressed as Equation (5)), and l is the pore-connectivity parameter, which is assumed to be 0.5.

$$\Theta = \frac{\theta - \theta_r}{\theta_s - \theta_r} \quad (5)$$

Average unsaturated hydraulic conductivity (\bar{K}) can be determined using the following equation:

$$\bar{K} = \frac{\int_{\theta_r}^{\theta_s} K(\theta) d\theta}{\theta_s - \theta_r} \quad (6)$$

2.4. Data Analysis

The retention curve code (RETC) program (Salinity Laboratory USAD, Riverside, CA, USA) was used to estimate the parameters of the SWCC and calculate the unsaturated hydraulic conductivity for each treatment. One-way analysis of variance (ANOVA) at the $\alpha = 0.05$ level of significance was adopted in SPSS 25 (IBM Corporation, New York, NY, USA). The least significant differences (LSD) test at the $\alpha = 0.05$ level of significance was conducted to analyze differences in the averages for the parameters related to infiltration and the SWCC, K_S , \bar{K} , and the averages of pH, EC, and the contents of Na^+ and Cl^- among treated water treatments (S1–S10) and the CK. Stepwise regressions and path analyses for infiltration parameters of the Philip equation, SWCC parameters of the VG model, K_S , \bar{K} , and average soil chemistry indicators in the 35 cm soil profile were performed using Excel 2016 (Microsoft Inc, Redmond, WA, USA). The coefficient of determination (R^2) and the

root mean square error (*RMSE*) were used to evaluate the accuracy of the Philip equation for infiltration and the VG model for the SWCC. The correlation coefficient (*r*) was used to evaluate the relationship between the two variables.

3. Results

3.1. Effect of Irrigation Salinity on Infiltration Characteristics of Red Soil

Similar trends of the relationship between cumulative infiltration and infiltration duration in red soil for UWI with five salinity levels (S1–S10) and the CK were found, showing that cumulative infiltration increased with an increase in infiltration duration (Figure 2). At the initial stage (0–25 min), as water infiltration is highly dependent on matric potential, no significant differences were detected in the cumulative infiltration among all treatments. This indicates that irrigation salinity had negligible influence on the cumulative infiltration of red soil at this stage. The cumulative infiltration for S1–S10 decreased by 8.61–41.18% compared with the CK. However, after the infiltration duration reached 25 min, salinity significantly decreased cumulative infiltration ($p < 0.05$) at the same time with the following order: CK > S1 > S5 > S2 > S3 > S10. It can also be concluded that irrigation salinity had a considerable impact on the infiltration rate of red soil. At the end of the experiment (i.e., when the wetting front reached 35 cm), the highest cumulative infiltration was found in the CK (14.8 cm), and S1–S10 decreased by 1.53–7.99%. Overall, UWI with 1–10 g L⁻¹ salinity could inhibit water infiltration and reduce water leaching at different degrees in red soil.

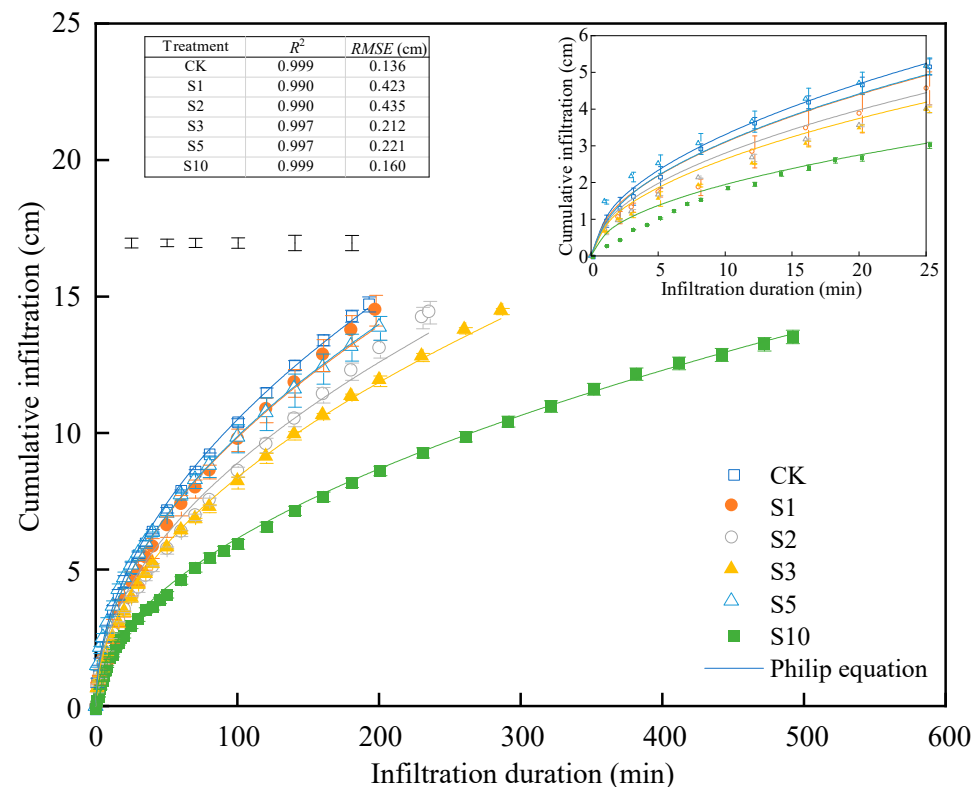


Figure 2. Cumulative infiltration with infiltration duration for UWI with different salinity levels (S1–S10) and CK in red soil. S1: 1 g L⁻¹; S2: 2 g L⁻¹; S3: 3 g L⁻¹; S5: 5 g L⁻¹; S10: 10 g L⁻¹; and CK: distilled water (0 g L⁻¹). The error bars represent the standard deviation. Error bars outside data points represent the LSD at 0.05 levels among treatments.

The Philip equation (Equation (1)) could well describe the relationship between cumulative infiltration and infiltration duration with $R^2 > 0.99$ and $RMSE < 0.44$ cm for all treatments (Figure 2). Compared to the CK (1.051 cm min^{-0.5}), UWI treatments significantly reduced *S* by 6.27–25.27% ($p < 0.05$), also supporting that UWI could inhibit the water

infiltration of red soil (Figure 3). Notably, S did not decrease monotonically with increasing salinity but showed a non-linear reduction. It declined initially to a minimum at S3 (0.839 cm min^{-0.5}), increased to a maximum at S5 (0.989 cm min^{-0.5}), and then decreased again to the lowest value at S10 (0.615 cm min^{-0.5}). It is worth noting that there was no significant difference in S between S1 and S5 ($p > 0.05$). As a result, there were two inflection points in the curve of salinity and S (S3 and S5). The relationship between irrigation salinity (C , g L⁻¹) and sorptivity (S , cm min^{-0.5}) can be well expressed with a cubic polynomial of irrigation salinity ($S = -0.004C^3 + 0.050C^2 - 0.184C + 1.095$, $R^2 = 0.952$).

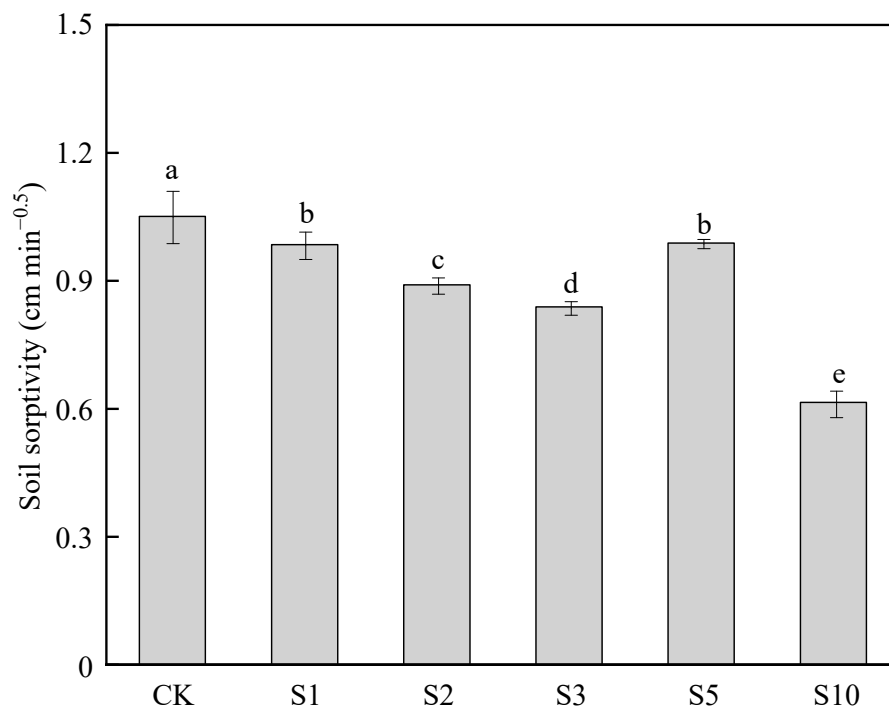


Figure 3. The soil sorptivity of Philip equation for UWI with different salinity levels (S1–S10) and CK in red soil. S1: 1 g L⁻¹; S2: 2 g L⁻¹; S3: 3 g L⁻¹; S5: 5 g L⁻¹; S10: 10 g L⁻¹; and CK: distilled water (0 g L⁻¹). Different letters indicate significant differences at $p < 0.05$. The error bars represent the standard deviation.

3.2. Effect of Irrigation Salinity on SWCC of Red Soil

The SWCC can be divided into three segments related to suction: a capillary segment (0–1020 cm), an adsorbed film segment (1.02 × 10³–10⁵ cm), and a tightly adsorbed segment (10⁵–10⁷ cm) [42]. The SWC decreased with an increase in soil water suction for all treatments (Figure 4). At the capillary segment, the shape of the SWCC was steep, illustrating that the soil water-holding capacity declined rapidly as soil water suction increased. At the adsorbed film segment, the curve became flat, signifying that changes in soil water suction did not result in a significant variation in the SWC. Moreover, the SWCC for S1, S3, and S5 shifted to the right of that for the CK, indicating that the water-holding capacity for S1, S3, and S5 was higher than that for the CK, and the highest was found in S5. In contrast, the SWCC for S2 and S10 were on the left of that for the CK, suggesting that the soil water-holding capacity for S2 and S10 was lower than that for the CK, and the lowest was found in S10.

Soil water constants obtained from the SWCC, including field capacity (FC) and permanent wilting point (PWP), were used to evaluate the effects of irrigation salinity on soil water-holding capacity in red soil (Table 2). S1–S5 significantly increased FC by 2.76–6.62% relative to the CK ($p < 0.05$), and the maximum value of the FC was observed in S3. However, there was no significant difference in FC between S10 and the CK ($p > 0.05$). These findings suggest that appropriate irrigation salinity could improve soil water-holding capacity. Furthermore, irrigation salinity also had a significant effect on the PWP ($p < 0.05$).

Specifically, S1, S3, and S5 dramatically increased the PWP by 1.53–5.06%, compared to the CK, and the maximum PWP was found in S5. In contrast, S10 had the lowest PWP, with a reduction of 3.94% compared to the CK ($p < 0.05$). As irrigation salinity had a positive influence on the FC and PWP, it could be difficult to generalize its effect on soil water availability. Therefore, soil available water capacity (SAWC: the difference between FC and PWP) was adopted to further assess the effects of the irrigation salinity. From Table 2, irrigation salinity considerably raised the SAWC. Compared with the CK, S1–S5 increased by 8.55–12.68% ($p < 0.05$), and the maximum SAWC was observed in S3 ($0.133 \text{ cm}^3 \text{ cm}^{-3}$). It is worth noting that although there was no significant difference in the SAWC between S10 and the CK ($p > 0.05$), S10 still had slightly higher SAWC than CK. These findings demonstrate that UWI could increase effective soil pores to improve the available water content of red soil contributing to plant biomass production.

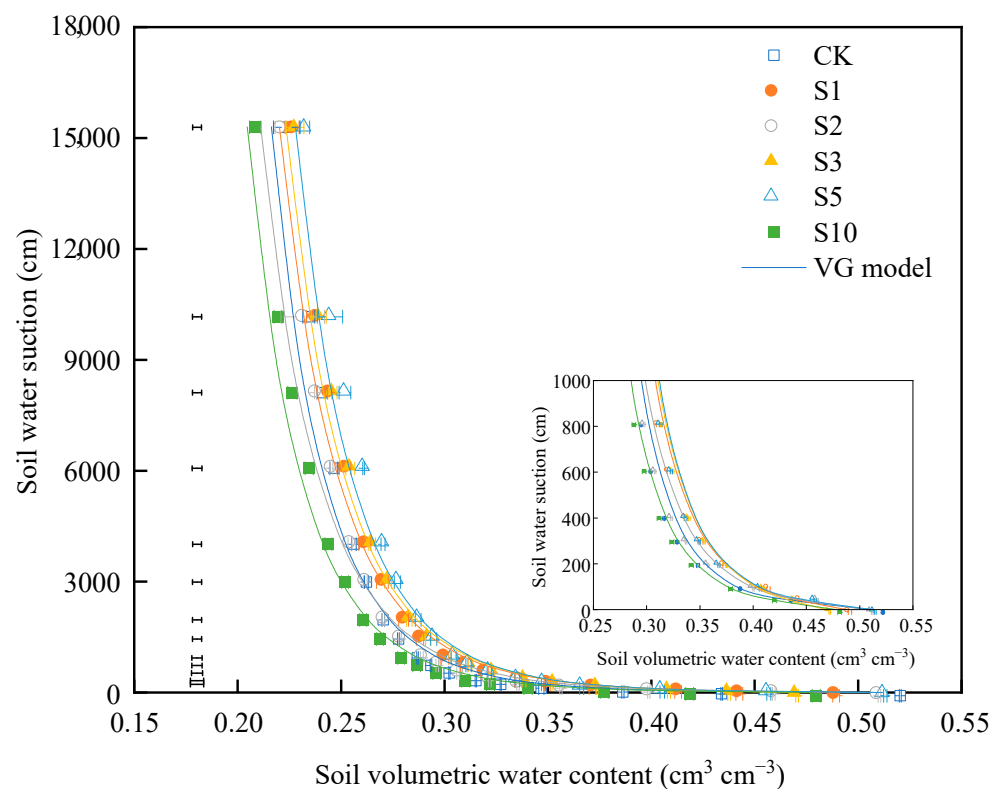


Figure 4. Soil water characteristic curve (SWCC) for UWI with different salinity levels (S1–S10) and CK in red soil. S1: 1 g L^{-1} ; S2: 2 g L^{-1} ; S3: 3 g L^{-1} ; S5: 5 g L^{-1} ; S10: 10 g L^{-1} ; and CK: distilled water (0 g L^{-1}). The error bars represent the standard deviation. Error bars outside data points represent the LSD at 0.05 levels among treatments.

Table 2. The parameters and performance of van Genuchten model and soil water constants for UWI with different salinity levels and CK.

Treatment	θ_s ($\text{cm}^3 \text{ cm}^{-3}$)	α (cm^{-1})	n	R^2	RMSE ($\text{cm}^3 \text{ cm}^{-3}$)	FC ($\text{cm}^3 \text{ cm}^{-3}$)	PWP ($\text{cm}^3 \text{ cm}^{-3}$)	SAWC ($\text{cm}^3 \text{ cm}^{-3}$)
CK	$0.512 \pm 0.016 \text{ ab}$	$0.142 \pm 0.019 \text{ a}$	$1.112 \pm 0.002 \text{ b}$	0.990	0.001	$0.335 \pm 0.002 \text{ c}$	$0.216 \pm 0.000 \text{ cd}$	$0.118 \pm 0.002 \text{ c}$
S1	$0.488 \pm 0.008 \text{ b}$	$0.049 \pm 0.002 \text{ cd}$	$1.122 \pm 0.004 \text{ a}$	0.990	0.001	$0.353 \pm 0.001 \text{ a}$	$0.220 \pm 0.004 \text{ bc}$	$0.133 \pm 0.003 \text{ a}$
S2	$0.509 \pm 0.006 \text{ a}$	$0.084 \pm 0.002 \text{ b}$	$1.123 \pm 0.002 \text{ a}$	0.989	0.001	$0.344 \pm 0.001 \text{ b}$	$0.213 \pm 0.003 \text{ de}$	$0.131 \pm 0.002 \text{ ab}$
S3	$0.469 \pm 0.010 \text{ c}$	$0.032 \pm 0.000 \text{ d}$	$1.122 \pm 0.005 \text{ a}$	0.993	0.001	$0.357 \pm 0.004 \text{ a}$	$0.223 \pm 0.002 \text{ ab}$	$0.134 \pm 0.006 \text{ a}$
S5	$0.511 \pm 0.006 \text{ a}$	$0.078 \pm 0.000 \text{ b}$	$1.115 \pm 0.003 \text{ ab}$	0.979	0.002	$0.356 \pm 0.000 \text{ a}$	$0.227 \pm 0.002 \text{ a}$	$0.128 \pm 0.003 \text{ ab}$
S10	$0.478 \pm 0.007 \text{ c}$	$0.067 \pm 0.001 \text{ bc}$	$1.120 \pm 0.001 \text{ ab}$	0.993	0.001	$0.331 \pm 0.003 \text{ c}$	$0.208 \pm 0.002 \text{ e}$	$0.123 \pm 0.002 \text{ bc}$

Different letters within a column indicate significant differences at $p < 0.05$. S1: 1 g L^{-1} ; S2: 2 g L^{-1} ; S3: 3 g L^{-1} ; S5: 5 g L^{-1} ; S10: 10 g L^{-1} ; and CK: distilled water (0 g L^{-1}).

The VG model can accurately represent the SWCC for UWI with different salinity levels (S1–S10) and the CK with $R^2 > 0.97$ and $RMSE < 0.002 \text{ cm}^3 \text{ cm}^{-3}$ (Table 2). Significant differences were found in VG model parameters (θ_s , α , and n) among UWI treatments and CK ($p < 0.05$). Generally, irrigation salinity reduced θ_s by 0.2–8.4%. θ_s for S3 and S10 were significantly lower than that for the CK with the lowest value of θ_s found in S3. Combined with the positive effects of irrigation salinity on the FC, PWP, and SAWC, it indicates that irrigation salinity could reduce the number of ineffective large soil pores in the red soil. Moreover, compared to CK, α was significantly decreased by 40.85–77.46% in S1–S10 ($p < 0.05$), showing that irrigation salinity increased the difficulty of initial drainage and the number of ineffective small soil pores. Additionally, higher n was detected in UWI treatments (S1–S10) with maximum n observed in S2, which also demonstrated that irrigation salinity could affect the soil pore structure of red soil.

3.3. Effect of Irrigation Salinity on Hydraulic Conductivity of Red Soil

K_S was reduced by 4.14–48.84% in red soil for UWI with different salinity levels (S1–S10) relative to the CK (Figure 5). Notably, K_S for S5 and S10 were significantly lower than that for the CK. Furthermore, there was a negative linear correlation between irrigation salinity and K_S ($R^2 = 0.837$), also providing evidence that irrigation salinity decreased the infiltration movement in red soil.

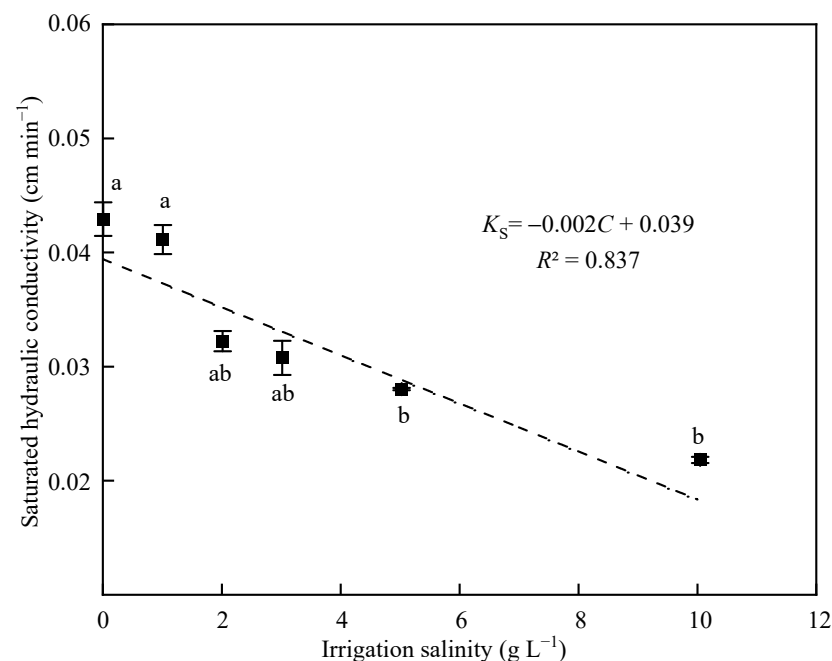


Figure 5. Saturated hydraulic conductivity of red soils for UWI with different salinity levels (S1–S10) and CK. S1: 1 g L⁻¹; S2: 2 g L⁻¹; S3: 3 g L⁻¹; S5: 5 g L⁻¹; S10: 10 g L⁻¹; and CK: distilled water (0 g L⁻¹). Different letters indicate significant differences at $p < 0.05$. The error bars represent the standard deviation.

The relationship between the SWC and K in red soil showed similar trends in UWI with different salinity levels (S1–S10) and the CK, with K decreasing rapidly as the SWC decreased (Figure 6a). When the SWC was lower than $0.40 \text{ cm}^3 \text{ cm}^{-3}$, the differences in K among UWI treatments and the CK were not significant. The negative influence of UWI on \bar{K} was evident and became more pronounced with increasing irrigation salinity (Figure 6b). Similar to K_S , in comparison to the CK, \bar{K} for S1–S10 also exhibited a substantial decrease by 13.98%, 18.81%, 24.07%, 39.48%, and 48.30%, respectively ($p < 0.05$). There was a significantly positive relationship between K_S and \bar{K} ($r = 0.943$, $p < 0.001$).

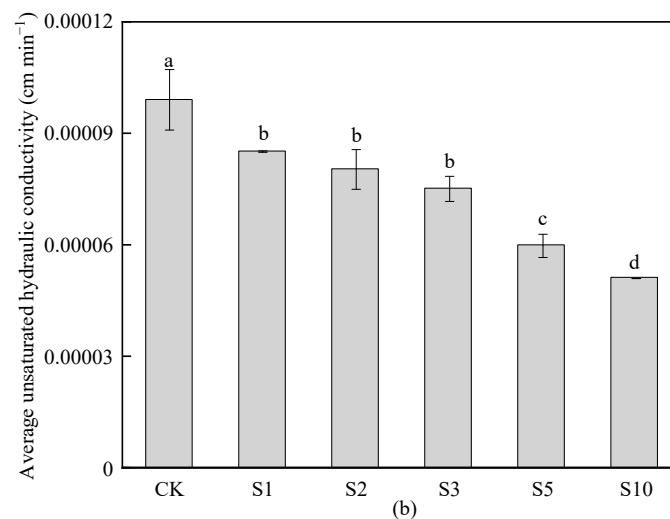
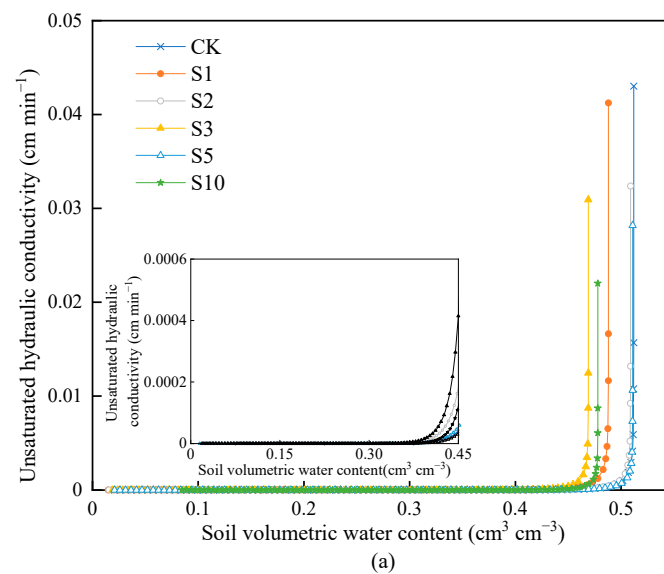


Figure 6. Unsaturated hydraulic conductivity with soil volumetric water content (a) and average unsaturated hydraulic conductivity (b) for UWI with different salinity levels (S1–S10) and CK in red soil. S1: 1 g L⁻¹; S2: 2 g L⁻¹; S3: 3 g L⁻¹; S5: 5 g L⁻¹; S10: 10 g L⁻¹; and CK: distilled water (0 g L⁻¹). Different letters indicate significant differences at $p < 0.05$. The error bars represent the standard deviation.

3.4. Effect of Irrigation Salinity on Salinity and pH of Red Soil

Irrigation salinity had a significant effect on soil salinity (EC, Na⁺, and Cl⁻ contents) and pH in the 0–35 cm soil profile ($p < 0.05$, Figure 7a–c). Compared to the CK, UWI treatments increased EC and Na⁺ and Cl⁻ contents in the 35 cm soil profile by 1.88–18.6, 3.13–23.3, and 4.56–70.7 times, which were far higher than the initial soil EC, Na⁺, and Cl⁻ contents, particularly in S10. It indicates that UWI could cause soil salinity accumulation in red soil. As irrigation salinity increased, the soil EC, Na⁺, and Cl⁻ contents increased linearly ($EC = 95.99C + 70.77$, $R^2 = 0.988$; $Na^+ = 0.119C + 0.091$, $R^2 = 0.992$; and $Cl^- = 0.136C - 0.020$, $R^2 = 0.970$). As for soil pH, S1–S5 treatments were reduced by 2.8–5.1% relative to CK. Soil pH for S2, S3, and S5 were significantly lower than CK ($p < 0.05$, Figure 7c). It should be noted that the soil for S5 was slightly higher than that for S1–S3 ($p > 0.05$), and the soil pH in CK was lower than the initial soil pH of 4.33, indicating that CK and S1–S5 could result in soil acidification, but S5 might slightly alleviate this phenomenon. Additionally, the maximum soil pH was observed in S10, which was significantly higher than that in the CK by 8.4%. The soil pH in S10 was also higher than the initial pH, demonstrating that higher irrigation salinity could cause soil alkalization

in red soil. As irrigation salinity increased, the soil pH decreased first and subsequently increased. There was a binomial relationship between soil pH and irrigation salinity ($\text{pH} = 0.0145C^2 - 0.109C + 4.11$, $R^2 = 0.992$).

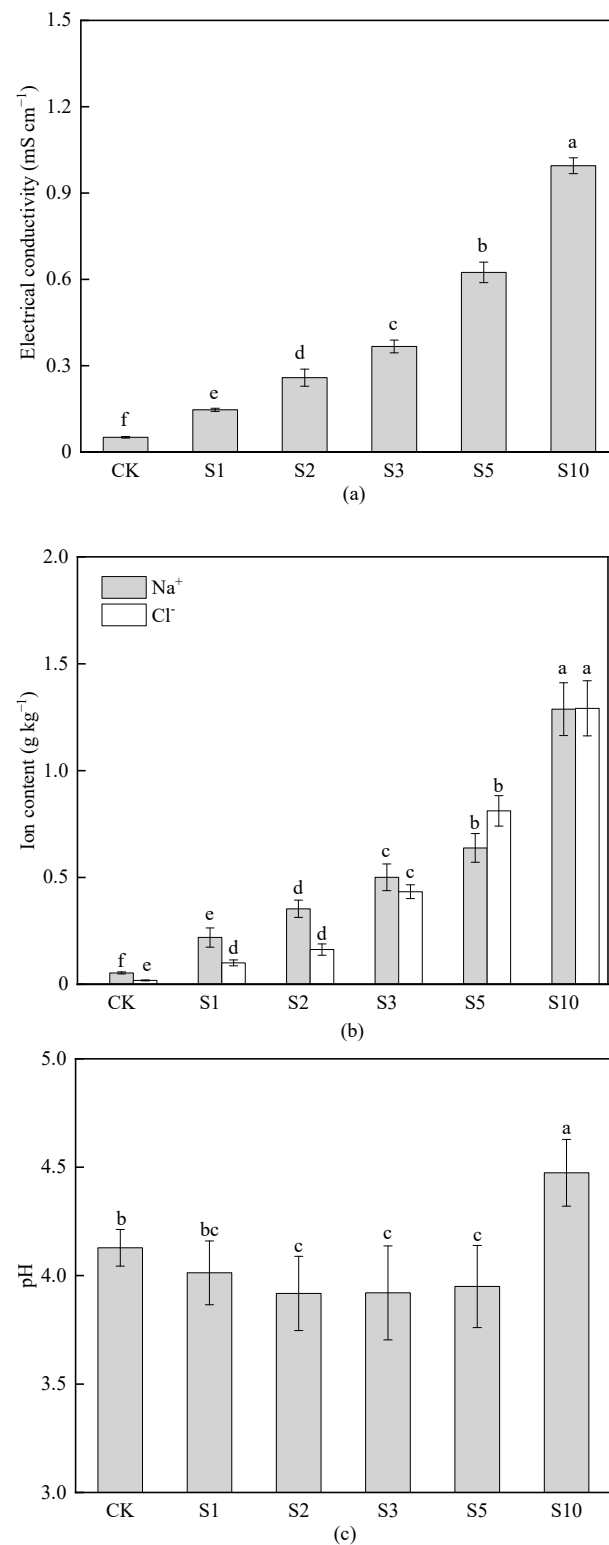


Figure 7. Electrical conductivity (a), ion content (b), and pH (c) for UWI with different salinity levels (S1–S10) and CK in red soil. S1: 1 g L⁻¹; S2: 2 g L⁻¹; S3: 3 g L⁻¹; S5: 5 g L⁻¹; S10: 10 g L⁻¹; and CK: distilled water (0 g L⁻¹). Different letters within a group indicate significant differences at $p < 0.05$. The error bars represent the standard deviation.

3.5. Relationship between Sorptivity and Its Correlative Parameters of Red Soil

A stepwise regression analysis was conducted to investigate the effects of irrigation salinity on water infiltration in red soil using S as a dependent variable to characterize the water infiltration. After eliminating collinear interference and higher correlation with S ($p < 0.05$), five parameters (θ_s , α , PWP, K_S , and EC) were adopted as independent variables to conduct stepwise regression. The regression model was as follows: $S = -1.294 + 11.782K_S + 7.869\text{PWP} + 1.151\alpha$ ($R^2 = 0.833$), indicating that α , PWP, and K_S were the main factors influencing water infiltration in red soil. Notably, these three variables exhibited a positive correlation with S with $r > 0.45$ (Table 3). The order of contribution to soil water infiltration was $K_S > \text{PWP} > \alpha$. Next, path analysis was used to further quantify the direct and indirect relationships between these three variables and S . These findings show that these three parameters (α , PWP, and K_S) had a positive influence on S , as their direct path coefficients were larger than zero, with the highest direct path coefficient of 0.591 for K_S . Additionally, the direct path coefficients of these three parameters were higher than the sum of their indirect path coefficients, demonstrating that there were larger direct contributions of these three parameters to water infiltration.

Table 3. Direct and indirect contributions of soil hydraulic properties and soil water constants on sorptivity (S) in red soil.

Variable	Correlation Coefficient	Direct Path Coefficient	The Sum of Indirect Path Coefficients	Indirect Diameter Coefficient		
				α	PWP	K_S
α	0.451	0.275	0.176	-	-0.070	0.245
PWP	0.552	0.455	0.097	-0.040	-	0.139
K_S	0.812	0.591	0.221	0.114	0.107	-

4. Discussion

4.1. Irrigation Salinity Inhibits Water Infiltration of Red Soil

Soil water infiltration could affect soil water utilization and plant growth. As freshwater resources are scarce, saline unconventional water can be used as a promising supplementary source for agricultural irrigation. Understanding the effect of the salinity of UWI on the water infiltration process can improve freshwater resource conservation, promote effective irrigation planning, and aid in the sustainable development of agriculture. In this study, a notable inhibition effect was found in cumulative infiltration in red soil under UWI with salinity levels ranging from 1 to 10 g L⁻¹ (S1–S10) in comparison to the CK (Figures 2 and 3), which is consistent with the previous research that reported a negative effect of irrigation salinity on water infiltration in red soil with reclaimed water irrigation (<1.66 mS cm⁻¹) [12].

Moreover, S obtained from the Philip equation (Equation (1)) was used to characterize the water infiltration process under UWI with different salinity levels (Figure 3). Similar to cumulative infiltration, UWI significantly reduced S , also indicating UWI had a negative influence on water flow in unsaturated red soil. However, different irrigation salinity levels yielded various degrees of negative effects. A greater reduction in water infiltration was observed with an increase in irrigation salinity within the range of 1 to 3 g L⁻¹ (S1–S3). This result is in agreement with Wu et al. [12] and Zhu et al. [18] who demonstrated that lower salinity of reclaimed water (<1.66 mS) reduced the cumulative infiltration in acid red soil. It could be attributed to three possible reasons. Firstly, Na⁺ accumulation from UWI (Figure 7b) could displace Mg²⁺ and Ca²⁺ on the soil surface, leading to soil shrinkage and colloid dispersion or swelling as well as the transformation of large soil particles into small soil particles [16,36], ultimately reducing the number of large pores and weakening water connectivity and fluidity in red soil [12]. This process could be aggravated as the irrigation salinity increases. Secondly, the displaced insoluble substances may accumulate in the soil column, blocking the path of water movement and decreasing soil water conductivity [12]. Indeed, K_S and \bar{K} decreased with an increase in irrigation salinity within a salinity of 3 (Figure 6). Additionally, from our previous study [43] and pH

in the 35 cm soil profile after UWI (Figure 7c), UWI with salinity levels ranging from 1 to 3 g L⁻¹ could induce soil acidification, resulting in damage to soil aggregate structure and stability [44]. Accordingly, soil water infiltration decreased as irrigation salinity increased within the range of 1 to 3 g L⁻¹. It is worth noting that *S* for S5 was still significantly lower than that for CK ($p < 0.05$), but it was greatly higher than S2 and S3 ($p < 0.05$) and not significantly different from S1 ($p > 0.05$). The one possible reason for higher *S* in S5 than in S2 and S3 is that the pH for S5 slightly increased compared to S2 and S3 and approached that for S1 (Figure 7c), which could overcome the negative effect of soil acidification on soil water infiltration. Additionally, the higher θ_s , FC, and PWP were found in S5, indicating that a larger pore volume could be present in this treatment. It could cause more water flow paths for infiltration in red soil, promoting soil water infiltration. Another possible reason is that α , the inverse of air-entry value, was higher for S5 than for S2 and S3, reflecting that S5 had a lower air-entry value than S2 and S3. It indicates that more drainage water could exist in S5 than in S2 and S3. Consequently, S5 had a larger cumulative infiltration, resulting in a higher *S* than S2 and S3 as well as a similar *S* to S1. By contrast, the highest reduction in soil water infiltration was found in S10, which can be accounted for by two factors. On one hand, soil alkalization was found in S10 with a higher pH than the initial (>4.33, Figure 7c), and Na⁺ acted as suspended solids that blocked the pores of soil particles preventing water movement and thus decreased water infiltration in red soil [45]. On the other hand, Na⁺ adsorbed by colloid in red soil may have reached its upper limit at the salinity level of 10 g L⁻¹, and the remaining Na⁺ could further disperse clay, destroying the structure and blocking the pores of the red soil [11,45–47], consequently resulting in the lowest water infiltration.

4.2. Irrigation Salinity Increases Soil Water Availability and Decreases the Hydraulic Conductivity of Red Soil

The SWCC is a fundamental tool for determining the hydraulic properties of unsaturated soil. Therefore, using the SWCC to illustrate the effect of irrigation salinity on hydraulic properties can help reveal the response of soil water infiltration to salinity. Irrigation salinity can affect the shape of the SWCC [19,48], particularly for the steepness of the SWCC, which shifts either to the left or right [48]. This present study determined that the SWCC shifted to the right in S1, S3, and S5, while it shifted to the left in S2 and S10 relative to the CK. The result in S5 is similar to the findings of Xing et al. [48] on loam soil from the Loess Plateau in China.

Furthermore, the VG model was used to quantify the effect of irrigation salinity on the SWCC. In this study, the parameters of the VG model (Equation (2), including θ_s , α , and n) and soil water constants (FC, PWP, and SAWC) estimated from the SWCC were used to elucidate the mechanism underlying the effect of irrigation salinity on water infiltration characteristics. From the present study, θ_s for S1 to S10 were lower than the CK, whereas the FC, PWP, and SAWC for S1 to S5 were generally higher than the CK. This could be attributed to the presence of NaCl, which enhanced clay flocculation and helped to form water stability aggregate structures under an irrigation salinity lower than 5 g L⁻¹, thereby increasing the number of effective soil pores in red soil. However, as irrigation salinity exceeded 5 g L⁻¹, salinity and ion accumulations occurred in the red soil (Figure 7a,b), occupying part of the original pore space and then causing large pores to gradually become smaller or even blocked, finally weakening the water-holding capacity of the red soil. This could also explain the increase in n . It is worth noting that n can reflect the slope and soil pore size distribution of the SWCC, and a larger n value indicates smaller pores could be found [39], indicating that UWI could reduce the number of ineffective large soil pores in the red soil. Furthermore, compared to the CK, higher FC, PWP, and SAWC for S1 to S5 were observed, which may be attributed to soil acidification (Figure 7c), leading to an increase in Cl⁻ adsorption (Figure 7b) and electrostatic potential energy among particles, ultimately restoring soil water and enhancing the water-holding capacity in red soil. This is also a possible reason for the increased difficulty in initial drainage and the reduction in α . In

contrast, the FC and PWP for S10 decreased compared to the CK, which is likely contributed by excessive Na^+ causing clay swelling and dispersion, producing more ineffective and dead soil pores [45,47,49], and reducing water-holding capacity. Additionally, S10 increased the pH of red soil (Figure 7c), possibly leading to a decline in electrostatic potential energy between red soil particles by reducing Cl^- adsorption capacity [50], thereby decreasing the water-holding capacity. Additionally, S1–S10 significantly reduced K_S and K of red soil, perhaps due to lower water transport capacity from the swelling/dispersion of clay particles and plugging of water passage, ultimately decreasing the hydraulic conductivity of red soil [49,51].

4.3. Key Factors Influencing Water Infiltration of Red Soil under UWI

Clarifying the factors that influence soil water infiltration is conducive to determining the appropriate water quality of supplementary irrigation water sources and improving agricultural irrigation plans. Additionally, optimizing the established model to predict the soil water infiltration process is a direction for further development. In the present study, we found that water infiltration characterized by S was mainly influenced by α , PWP, and K_S under UWI, with a contribution order of $K_S > \text{PWP} > \alpha$. K_S is a key parameter that reflects soil hydraulic characteristics [52,53], with a larger K_S indicating a stronger water transport capacity of the soil, and a higher K_S could lead to rapid water flow. Youngs [54] proposed an equation suggesting that sorptivity mainly depends on K and θ_i . Our results are in agreement with the previous results of Wang et al. [24,27] and Huo and Jin [25] that K_S had a significant contribution to soil water infiltration. Moreover, some previous studies [26,28] reported that a strong correlation between K_S and α was found. According to the previous studies [25,28,29] on the parameter sensitivity of the VG model on infiltration, infiltration can be significantly affected by K_S and α . These similar results could support that the soil water infiltration under UWI can be influenced by α of the VG model from our present study. In our present study, a significant correlation between K_S and α was also observed ($r = 0.414$, $p < 0.05$), indicating that α as a key factor can influence soil water infiltration. As for PWP, there is little study on its effect on water movement. However, some studies reported that PWP is primarily influenced by soil clay contents, and the soil with higher clay content has a higher PWP. It indicates that soil water infiltration under UWI could be related to soil clay content and that UWI can influence soil porosity in red soil. Basile et al. [11] found soil pore redistribution in saline treatment using image analysis and demonstrated that the number of soil pores larger than $36 \mu\text{m}$ decreased, while new soil pores with size of 2500 and $3200 \mu\text{m}$ emerged in saline soils. It could also explain that higher S was found in S5 than in S2 and S3. Therefore, the effects of UWI on soil pore distribution should be further investigated. Additionally, it should be noted that the three variables (α , PWP, and K_S) only explain 83.3% of S . The possible reason is that the number of treatments in this study is less, and these three variables could not represent the variation in S with different salinity levels. More salinity levels (such as 4 and 8 g L^{-1}) could be added to help validate and support this conclusion.

5. Conclusions

In this study, we analyzed the effects of irrigation salinity on cumulative infiltration behavior, hydraulic parameters (SWCC, K_S , and K), soil water constants (θ_s , FC, PWP, and SAWC) in red soil based on the Philip equation and VG model. We also identified the key factors influencing water infiltration of red soil using stepwise regression and path analysis. Our findings demonstrate that irrigation salinity can inhibit the water infiltration of red soil, and the cumulative infiltration was followed as $\text{CK} > \text{S1} > \text{S5} > \text{S2} > \text{S3} > \text{S10}$. At the end of infiltration, S1–S10 decreased cumulative infiltration by 1.53–7.99%. Moreover, there was a cubic relationship between irrigation salinity and soil sorptivity from the Philip equation. The VG model can describe the SWCC for UWI with different salinity levels. Irrigation salinity increased soil water availability by 8.55–12.68%. Notably, irrigation salinity significantly reduced K_S and K of red soil, and a negative linear relationship was

observed between irrigation salinity and K_s . Moreover, UWI can cause salinity and ion accumulation in the soil profile, and there was a positively linear relationship between salinity accumulation and irrigation salinity. Soil acidification was found in S1–S5, and soil alkalization was found in S10. Additionally, α , PWP, and K_s were recognized as key factors affecting water infiltration in red soil. Our study can provide a reference for supplementary UWI in red soil. It should be noted there is a risk of salinization associated with UWI. However, considering the elimination of inter-ion effects under UWI and the heterogeneity of soil, this study was based on disturbed red soil and simulated water of limited salinity, which could not fully represent the actual condition. Therefore, further study on undisturbed or in situ red soil under agricultural unconventional water irrigation should be considered. Additionally, to assess the sustainability of unconventional water applications, it is also necessary to conduct further long-term studies.

Author Contributions: Conceptualization, S.T., S.C. and Q.Y.; methodology, S.T., X.S. and X.J.; software, X.S., X.J. and W.Y.; validation, Q.Y. and S.N.; formal analysis, S.T., X.S., X.J. and S.N.; investigation, X.S., X.J. and W.Y.; data curation, X.S. and X.J.; writing—original draft preparation, X.S. and X.J.; writing—review and editing, S.T., S.C. and S.N.; visualization, S.T. and X.S.; supervision, S.C., Q.Y. and S.N.; funding acquisition, S.T., S.C. and Q.Y. All authors have read and agreed to the published version of the manuscript.

Funding: This research was funded by the National Natural Science Foundation of China grant numbers [52009039 and 52209056], the Yunnan Fundamental Research Projects [202301AU070190 and 202301AU070095]; the Yunnan Provincial Field Scientific Observation and Research Station on Water-Soil-Crop System in Seasonal Arid Region [202305AM070006]; A Project Supported by Scientific Research Fund of Hunan Provincial Education Department (Grant No. 18C0156); the Natural Science Foundation of Xinjiang Uygur Autonomous Region [2022D01B70], the Yunnan Science and Technology Talent and Platform Program [202305AM070006], the Key Laboratory Project of Efficient Water Use and Green Production of Specialty Crops in Yunnan Universities [KKPS201923009], and the Scientific Research Fund Project of Yunnan Provincial Department of Education [2022D01B70].

Data Availability Statement: The data used to support the findings of this study are included within the article.

Acknowledgments: We thank Hui Wang and Fengping Wu of the Hunan Agricultural University for their help in the experiment.

Conflicts of Interest: The authors declare no conflict of interest.

References

- Gao, W.; Xue, L.; Liu, L.; Lu, C.; Yun, Y.; Zhou, W. A study of the fraction of warm rain in a pre-summer rainfall event over South China. *Atmos. Res.* **2021**, *262*, 105792. [[CrossRef](#)]
- Li, W.; Zhao, S.; Chen, Y.; Wang, L.; Hou, W.; Jiang, Y.; Zou, X.; Shi, S. State of China's climate in 2021. *Atmos. Ocean. Sci. Lett.* **2022**, *15*, 100211. [[CrossRef](#)]
- Zhang, M.; Xu, J. Restoration of surface soil fertility of an eroded red soil in southern China. *Soil Tillage Res.* **2005**, *80*, 13–21. [[CrossRef](#)]
- Adeyemo, T.; Kramer, I.; Levy, G.J.; Mau, Y. Salinity and sodicity can cause hysteresis in soil hydraulic conductivity. *Geoderma* **2022**, *413*, 115765. [[CrossRef](#)]
- Oster, J. Irrigation with poor quality water. *Agric. Water Manag.* **1994**, *25*, 271–297. [[CrossRef](#)]
- Li, J.; Chen, J.; He, P.; Chen, D.; Dai, X.; Jin, Q.; Su, X. The optimal irrigation water salinity and salt component for high-yield and good-quality of tomato in Ningxia. *Agric. Water Manag.* **2022**, *274*, 107940. [[CrossRef](#)]
- Brewster, M.R.; Buros, O.K. The use of non-conventional water resource alternatives in water short areas. *Desalination* **1985**, *56*, 89–108. [[CrossRef](#)]
- Amori, P.N.; Mierzwa, J.C.; Bartelt-Hunt, S.; Guo, B.; Saroj, D.P. Germination and growth of horticultural crops irrigated with reclaimed water after biological treatment and ozonation. *J. Clean. Prod.* **2022**, *336*, 130173. [[CrossRef](#)]
- Mendoza-Espinosa, L.G.; Burgess, J.E.; Daesslé, L.; Villada-Canela, M. Reclaimed water for the irrigation of vineyards: Mexico and South Africa as case studies. *Sustain. Cities Soc.* **2019**, *51*, 101769. [[CrossRef](#)]
- Karimidastenaei, Z.; Avellán, T.; Sadegh, M.; Kløve, B.; Haghighi, A.T. Unconventional water resources: Global opportunities and challenges. *Sci. Total Environ.* **2022**, *827*, 154429. [[CrossRef](#)]
- Basile, A.; Buttafuoco, G.; Mele, G.; Tedeschi, A. Complementary techniques to assess physical properties of a fine soil irrigated with saline water. *Environ. Earth Sci.* **2012**, *66*, 1797–1807. [[CrossRef](#)]

12. Wu, Y.; Wang, H.; Zhu, J. Influence of reclaimed water quality on infiltration characteristics of typical subtropical zone soils: A case study in South China. *Sustainability* **2022**, *14*, 4390. [[CrossRef](#)]
13. Li, J.; Gao, Y.; Zhang, X.; Tian, P.; Li, J.; Tian, Y. Comprehensive comparison of different saline water irrigation strategies for tomato production: Soil properties, plant growth, fruit yield and fruit quality. *Agric. Water Manag.* **2019**, *213*, 521–533. [[CrossRef](#)]
14. Zhang, H.; Wang, J.; Lei, Y. Research on soil desalinization through platform fields and by irrigation using sea-ice water. In Proceedings of the 19th World Congress of Soil Science: Soil Solutions for a Changing World, Brisbane, Australia, 1–6 August 2010.
15. Cao, D.; Shi, B.; Wei, G.; Chen, S.; Zhu, H. An improved distributed sensing method for monitoring soil moisture profile using heated carbon fibers. *Measurement* **2018**, *123*, 175–184. [[CrossRef](#)]
16. Tarchouna, L.G.; Merdy, P.; Raynaud, M.; Pfeifer, H.; Lucas, Y. Effects of long-term irrigation with treated wastewater. Part I: Evolution of soil physico-chemical properties. *Appl. Geochem.* **2010**, *25*, 1703–1710. [[CrossRef](#)]
17. Zhang, P.; Shen, J. Effect of brackish water irrigation on the movement of water and salt in salinized soil. *Open Geosci.* **2022**, *14*, 404–413. [[CrossRef](#)]
18. Zhu, J.; Wang, H.; Hu, C.; Liu, C.; Chen, X. The Change in hydraulic conductivity of red soil irrigated with treated wastewater. *J. Irrig. Drain.* **2019**, *38*, 64–69. (In Chinese with English abstract).
19. Rezaei, M.; Shahbazi, K.; Shahidi, R.; Davatgar, N.; Bazargan, K.; Rezaei, H.; Saadat, S.; Seuntjens, P.; Cornelis, W. How to relevantly characterize hydraulic properties of saline and sodic soils for water and solute transport simulations. *J. Hydrol.* **2021**, *598*, 125777. [[CrossRef](#)]
20. Chaudhari, S. Saturated hydraulic conductivity, dispersion, swelling, and exchangeable sodium percentage of different textured soils as influenced by water quality. *Commun. Soil Sci. Plant Anal.* **2001**, *32*, 2439–2455. [[CrossRef](#)]
21. Amini, M.; Ebrahimian, H.; Liaghat, A.; Fujimaki, H. Unsaturated soil hydraulic properties according to double-ring infiltration of saline water. *Eurasian Soil Sci.* **2020**, *53*, 1596–1609. [[CrossRef](#)]
22. Chen, X.; Shen, Q.; Xu, Y. Hydraulic properties of typical salt-affected soils in Jiangsu Province, China. *Front. Environ. Sci. Eng. China* **2007**, *1*, 443–447. [[CrossRef](#)]
23. Fan, Y.; Zhu, C.; Bai, G.; Ma, T.; Wang, Z. Numerical simulation of soil water movement by gravity subsurface hole irrigation. *Water Supply* **2022**, *22*, 6389–6404. [[CrossRef](#)]
24. Wang, Z.; Jiao, X.; Han, H.; Yu, X. Sensitivity analysis of VG model parameters with vertical one-dimensional soil infiltration. *J. Hohai Univ. (Nat. Sci.)* **2013**, *41*, 80–84. (In Chinese with English abstract)
25. Huo, S.; Jin, M. Effect of parameter sensitivity of van genuchten model on numerical simulation of rainfall recharge. *Earth Sci.* **2017**, *42*, 447–452+470. (In Chinese with English abstract).
26. Stothoff, S.A. Sensitivity of long-term bare soil infiltration simulations to hydraulic properties in an arid environment. *Water Resour. Res.* **1997**, *33*, 547–558. [[CrossRef](#)]
27. Wang, Z.; Feyen, J.; van Genuchten, M.T.; Nielsen, D.R. Air entrapment effects on infiltration rate and flow instability. *Water Resour. Res.* **1998**, *34*, 213–222. [[CrossRef](#)]
28. Pan, F.; Zhu, J.; Ye, M.; Pachepsky, Y.A.; Wu, Y.S. Sensitivity analysis of unsaturated flow and contaminant transport with correlated parameters. *J. Hydrol.* **2011**, *397*, 238–249. [[CrossRef](#)]
29. Maina, F.Z.; Siirila-Woodburn, E.R. The role of subsurface flow on evapotranspiration: A global sensitivity analysis. *Water Resour. Res.* **2020**, *56*, e2019WR026612. [[CrossRef](#)]
30. Bezborodov, G.A.; Shadmanov, D.K.; Mirhashimov, R.T.; Yuldashev, T.; Qureshi, A.S.; Noble, A.D.; Qadir, M. Mulching and water quality effects on soil salinity and sodicity dynamics and cotton productivity in Central Asia. *Agric. Ecosyst. Environ.* **2010**, *138*, 95–102. [[CrossRef](#)]
31. Guo, X.; Du, S.; Guo, H.; Min, W. Long-term saline water drip irrigation alters soil physicochemical properties, bacterial community structure, and nitrogen transformations in cotton. *Appl. Soil Ecol.* **2023**, *182*, 104719. [[CrossRef](#)]
32. Dong, X.; Wang, J.; Zhang, X.; Dang, H.; Singh, B.P.; Liu, X.; Sun, H. Long-term saline water irrigation decreased soil organic carbon and inorganic carbon contents. *Agric. Water Manag.* **2022**, *270*, 107760. [[CrossRef](#)]
33. Yang, G.; Li, F.; Tian, L.; He, X.; Gao, Y.; Wang, Z.; Ren, F. Soil physicochemical properties and cotton (*Gossypium hirsutum* L.) yield under brackish water mulched drip irrigation. *Soil Tillage Res.* **2020**, *199*, 104592. [[CrossRef](#)]
34. Cheng, M.; Wang, H.; Fan, J.; Wang, X.; Sun, X.; Yang, L.; Zhang, S.; Xiang, Y.; Zhang, F. Crop yield and water productivity under salty water irrigation: A global meta-analysis. *Agric. Water Manag.* **2021**, *256*, 107105. [[CrossRef](#)]
35. Hopmans, J.W.; Qureshi, A.S.; Kisekka, I.; Munns, R.; Grattan, S.R.; Rengasamy, P.; Ben-Gal, A.; Assouline, S.; Javaux, M.; Minhas, P.S.; et al. Critical knowledge gaps and research priorities in global soil salinity. *Adv. Agron.* **2021**, *169*, 1–191.
36. Heydari, N.; Gupta, A.D.; Loof, R. Salinity and sodicity influences on infiltration during surge flow irrigation. *Irrig. Sci.* **2001**, *20*, 165.
37. Zhang, J.; Wang, Q.; Shan, Y.; Guo, Y.; Mu, W.; Wei, K.; Sun, Y. Effect of sodium carboxymethyl cellulose on water and salt transport characteristics of saline-alkali soil in Xinjiang, China. *Polymers* **2022**, *14*, 2884. [[CrossRef](#)]
38. Philip, J. The theory of infiltration: 1. The infiltration equation and its solution. *Soil Sci.* **1957**, *83*, 345–358. [[CrossRef](#)]
39. van Genuchten, M.T. A closed-form equation for predicting the hydraulic conductivity of unsaturated soils. *Soil Sci. Soc. Am. J.* **1980**, *44*, 892–898. [[CrossRef](#)]
40. Darcy, H. *Les Fontaines Publiques de la ville de Dijon: Exposition et Application des Principes à Suivre et des Formules à Employer dans les Questions de Distribution d'eau*; Victor Dalmont: Paris, France, 1856; Volume 1.

41. Mualem, Y. A new model for predicting the hydraulic conductivity of unsaturated porous media. *Water Resour. Res.* **1976**, *12*, 513–522. [[CrossRef](#)]
42. McQueen, I.S.; Miller, R.F. Approximating soil moisture characteristics from limited data: Empirical evidence and tentative model. *Water Resour. Res.* **1974**, *10*, 521–527. [[CrossRef](#)]
43. Jiang, X.; Wu, F.; Tan, S.; Wang, H.; Song, C.; Chen, T.; Li, Q.; Meng, Z. The effects of concentration of ponding-infiltration water on water and salt movement in soils. *J. Irrig. Drain.* **2021**, *40*, 81–88. (In Chinese with English abstract)
44. Polanía-Hincapié, K.L.; Olaya-Montes, A.; Cherubin, M.R.; Herrera-Valencia, W.; Ortiz-Morea, F.A.; Silva-Olaya, A.M. Soil physical quality responses to silvopastoral implementation in Colombian Amazon. *Geoderma* **2021**, *386*, 114900. [[CrossRef](#)]
45. Amer, A.M. Prediction of hydraulic conductivity and sorptivity in soils at steady-state infiltration. *Arch. Agron. Soil Sci.* **2012**, *58*, 1179–1194. [[CrossRef](#)]
46. She, D.; Gao, X.; Peng, W.; Xu, W.; Liu, Y.; Liu, Y. Comparison of soil hydraulic properties with different levels of soil salinity and sodicity. *Arab. J. Geosci.* **2015**, *8*, 5351–5360.
47. Higashino, M.; Erickson, A.J.; Toledo-Cossu, F.L.; Beauvais, S.W.; Stefan, H.G. Rinsing of saline water from road salt in a sandy soil by infiltrating rainfall: Experiments, simulations, and implications. *Water Air Soil Pollut.* **2017**, *228*, 80. [[CrossRef](#)]
48. Xing, X.; Kang, D.; Ma, X. Differences in loam water retention and shrinkage behavior: Effects of various types and concentrations of salt ions. *Soil Tillage Res.* **2017**, *167*, 61–72. [[CrossRef](#)]
49. Bagarello, V.; Iovino, M.; Palazzolo, E.; Panno, M.; Reynolds, W. Field and laboratory approaches for determining sodicity effects on saturated soil hydraulic conductivity. *Geoderma* **2006**, *130*, 1–13. [[CrossRef](#)]
50. Zhang, X.; Jiang, N.; Shao, Z.; Pan, S.; Zhang, W. Studies on electrochemical properties of soils VI. Adsorption of ions by red soils in relation to the electric charge of the soil. *Acta Pedol. Sin.* **1979**, *16*, 145–156. (In Chinese with English abstract)
51. Tedeschi, A.; Dell’Aquila, R. Effects of irrigation with saline waters, at different concentrations, on soil physical and chemical characteristics. *Agric. Water Manag.* **2005**, *77*, 308–322. [[CrossRef](#)]
52. Zhang, R. Determination of soil sorptivity and hydraulic conductivity from the disk infiltrometer. *Soil Sci. Soc. Am. J.* **1997**, *61*, 1024–1030. [[CrossRef](#)]
53. Usowicz, B.; Lipiec, J. Spatial variability of saturated hydraulic conductivity and its links with other soil properties at the regional scale. *Sci. Rep.* **2021**, *11*, 8293. [[CrossRef](#)] [[PubMed](#)]
54. Youngs, E.G. The measurement of the variation with depth of the hydraulic conductivity of saturated soil monoliths. *J. Soil Sci.* **1982**, *33*, 3–12. [[CrossRef](#)]

Disclaimer/Publisher’s Note: The statements, opinions and data contained in all publications are solely those of the individual author(s) and contributor(s) and not of MDPI and/or the editor(s). MDPI and/or the editor(s) disclaim responsibility for any injury to people or property resulting from any ideas, methods, instructions or products referred to in the content.